

# Galaxy Zoo Builder: Morphological Dependence of Spiral Galaxy pitch angle

Timothy Lingard<sup>1\*</sup>, Karen L. Masters<sup>2</sup>, Coleman Krawczyk<sup>1</sup>, Robert C. Nichol,<sup>1</sup>

<sup>1</sup>*Institute of Cosmology and Gravitation, University of Portsmouth, Dennis Sciama Building, Burnaby Road, Portsmouth, PO1 3FX, UK*

<sup>2</sup>*Haverford College, 370 Lancaster Ave., Haverford, PA 19041, USA*

Accepted XXX. Received YYY; in original form ZZZ

## ABSTRACT

Abstract

**Key words:** galaxies: evolution – galaxies: spiral – galaxies: photometry

## 1 INTRODUCTION

Spiral structure is present in a majority of massive galaxies (Buta 1989, Lintott et al. 2008) yet the formation mechanisms through which spiral structure originates are still hotly debated. Spirals are as diverse as the theories proposed to govern their evolution; from the quintessential pair of well-defined arcs of the grand design spiral, to the fragmented arm segments of the flocculent spiral, to the disjointed multi-armed spiral. These variations on structure account for 18%, 50% and 32% of the population respectively (Elmegreen et al. 2011, Buta et al. 2015). The Hubble classification scheme (Hubble 1926), and its revisions and expansions (Sandage 1961, de Vaucouleurs et al. 1991) contain detailed variations of different types of spiral galaxy, divided by the presence of a bar and ordered by how obvious spiral arm patterns are, how tightly they are wound and the prominence of a central bulge.

Arms of spiral galaxies are the source of the vast majority of star formation in the Universe, and spirals rearrange disc gas and can lead to the formation of disc-like bulges (e.g. Kormendy & Kennicutt 2004). Studies of spiral morphology have found interesting correlations between spiral morphology and other galactic properties, such as a correlation between spiral tightness and central mass concentration (Yu & Ho 2019, Davis 2015, though Hart et al. 2017 found no such relation) and tightness and rotation curve shape (Seigar et al. 2005, with rising rotation curves creating more open spiral structure). These predictions and observations provide compelling reasons for investigating their underlying rules and dynamics, as doing so is essential for understanding the secular evolution of disc galaxies.

Our current understanding of the mechanisms which drive spiral growth and evolution suggest that each of the different forms of spiral galaxy may be triggered primarily by different processes. Grand Design spirals are thought to

have undergone a tidal interaction, be driven by a bar (as seen in gas simulations, Sanders & Huntley 1976, Rodriguez-Fernandez & Combes 2008, and suggested for stars by Manifold theory, Romero-Gómez et al. 2006, Athanassoula et al. 2009a, Athanassoula et al. 2009b), or be obeying (quasi-stationary) density wave theory (QSDW theory), in which spiral arms are slowly evolving, ever-present structures in the disc (Lin & Shu 1964). Flocculent spirals are thought to be formed through swing amplification (shearing of small gravitational instabilities in the disc), and be transient and recurrent in nature (Julian & Toomre 1966). It is recognised that methods of spiral formation are not mutually exclusive.

One of the fundamental assumptions of early work on spiral formation mechanisms (primarily QSDW) was that the disc of a galaxy, if unstable to spiral perturbations, would create a stable, static wave which would exist unchanging for many rotational periods (Lin & Shu 1964). The motivation for static waves with small numbers of arms (with a preference for  $m = 2$ ) was primarily observational; most galaxies show spiral structure, suggesting that spirals exist for a long time or are continually rebuilt.

Many simulations demonstrate that spirals do not maintain a constant pitch angle, and instead wind-up over time due to the differential rotation of the disc (Baba et al. 2013). Recent research suggests that spirals are dynamical in nature, and continually dissipate and re-form (Dobbs & Baba 2014). These spirals can be maintained through the same mechanisms that drive QSDW spirals (i.e. WASER, Mark 1976, swing amplification, Goldreich & Lynden-Bell 1965), but do not require the idealistic disc conditions required for the formation and maintenance of a stationary wave. The pitch angles of these transient spiral arms will decrease due to the differential rotation of the disc, with the density of the arm peaking at some critical pitch angle and then dissipating to be reformed.

In this dynamic picture of spiral arms, pitch angle monotonically decreases from a spiral arm's formation to its dissipation. Pringle & Dobbs (2019) proposes a simple

\* E-mail: tim.lingard@port.ac.uk

test of spiral arm winding, assuming the cotangent of the pitch angle of a spiral arm evolves linearly with time. They found that the pitch angles of their sample of 86 galaxies was consistent with this distribution, evidence against QSDW theory in favour of the dynamic spirals produced in many simulations.

Spiral evolution also appears to be influenced by the presence and strength of a bar; in barred grand-design spirals the arms often appear to start from the ends of the bar. Simulations of gas in barred galaxies often demonstrate that bars can drive long-term spiral evolution (Rodríguez-Fernández & Combes 2008), or boost transient spiral structure (Grand et al. 2012). Manifold theory is one attempt to determine the orbits of stars in bar-driven spiral arms: it proposes that stars in the vicinity of the unstable Lagrangian points at either end of the bar tend to escape along predictable orbits, governed by invariant manifolds. One of the primary factors influencing the shape of this invariant manifold is the relative strength of the non-axisymmetric forcing caused by the bar, with stronger bars resulting in spirals with larger pitch angles.

Many other systems contribute to spiral morphology, including potential ties to bulge fraction (Yoshizawa & Wakamatsu 1975, Savchenko & Reshetnikov 2013, Masters et al. 2019) and black hole mass (Davis 2015, Davis et al. 2017), via a series of correlations. Stronger bulges and more massive central black holes have both been linked to more tightly wound spiral arms.

This paper makes use of the classification data and fitted photometric models obtained through the *Galaxy Builder* citizen science project for the 196 spiral galaxies present in [\[Lingard et al. \(2020\)\]](#). In this paper we focus on the use of measured spiral tightness (quantified using pitch angle, Binney & Tremaine 1987) as a probe into the dynamical mechanisms governing a spiral galaxy’s evolution. We make use of Bayesian hierarchical modelling to measure galaxy pitch angle from the spiral arm clusters produced by *Galaxy Builder*.

Section 3.3 investigates spiral arm winding using the test derived by Pringle & Dobbs (2019) (uniformity of galaxy pitch angle in  $\cot \phi$ ) and concludes using a marginalized Anderson-Darling test that we cannot unilaterally reject winding of this form at the 1% level. Section 3.2 examines the correlation between pitch angle and bulge size implied by the Hubble sequence, and pitch angle and bar strength implied by Manifold theory, and find no significant correlation.

## 2 METHOD

### 2.1 Measuring galaxy pitch angle

Many methodologies have been proposed and implemented to measure spiral arm properties, including visual inspection (Herrera-Endoqui et al. 2015), fourier analysis (i.e. 2DFFT, Davis et al. 2012), texture analysis (i.e. SpArcFiRe, Davis & Hayes 2014), and combinations of automated methods and human classifiers (Hart et al. 2017, Hewitt & Treuthardt 2020). One potentially underused method of obtaining measurements of spirals is through photometric fitting of spiral structure, as possible using tools such as GALFIT (Peng

et al. 2010) and *Galaxy Builder* ([\[Lingard et al. \(2020\)\]](#)). These methods attempt to localize light from an image of a galaxy into distinct subcomponents, such as a galaxy disc, bulge, bar and spiral arms, generally finding the optimum solution using computational optimization. This optimization process, however, is often not robust for complex, many-component models and requires significant supervision to converge to a physically meaningful result (Gao & Ho 2017). [\[Lingard et al. \(2020\)\]](#) propose a solution to this problem through the use of citizen science to provide priors on parameters used in computational fitting.

A common assumption when measuring galaxy pitch angle is that observed spiral arms have a constant pitch angle. Spirals of this kind are known as logarithmic spirals and are described by

$$r = A e^{\theta \tan \phi}, \quad (1)$$

where  $\phi$  is the arm’s pitch angle. One method used to obtain a pitch angle of a galaxy is to fit logarithmic spirals to individually identified arm segments and take the weighted mean of their pitch angles (which often vary by upwards of  $10^\circ$ , Davis & Hayes 2014). Weighting is determined by the length of the arc segment, with longer being assigned higher weights, i.e. for a galaxy where we have identified  $N$  arm segments, each with length  $L_i$  and pitch angle  $\phi_i$

$$\phi_{\text{gal}} = \left( \sum_{i=1}^N L_i \right)^{-1} \sum_{i=1}^N L_i \phi_i. \quad (2)$$

The most commonly used measurement of uncertainty of length-weighted pitch angles is the unweighted sample variance between the arm segments identified.

A notable drawback of length-weighted pitch angle is sensitivity to the number and quality of the spiral arm segments identified; Hart et al. (2017) found that only 15% of the arm segments identified by a leading algorithm (SPARCFIRE) were identified as “good” matches to real spiral arms by citizen science classifiers.

Fourier analysis in one- and two-dimensions (as performed by Díaz-García et al. 2019, Davis et al. 2012, Mutlu-Pakdil et al. 2018) is another widely used method of computationally obtaining galaxy pitch angles. Two-dimensional fourier methods generally decompose a deprojected image of a galaxy into a superpositions of logarithmic spirals between inner and outer annuli (Davis et al. 2012), and reports the pitch angle with the highest amplitude as the galaxy’s pitch angle. Hewitt & Treuthardt (2020) combined fourier analysis of spiral galaxies with human tracing of spiral arms, to great effect. It is uncertain how variation between pitch angles of individual arms impacts this measurement.

### 2.2 The Galaxy Sample

The galaxies analysed in this paper are the 198 galaxies from [\[Lingard et al. \(2020\)\]](#). These are a subset of the *stellar mass-complete sample* in Hart et al. (2017), a sample of low-redshift face-on spiral galaxies selected using data from the NASA-Sloan Atlas (Blanton et al. 2011) and Galaxy Zoo 2 (Willett et al. 2013).

Some galaxies in [\[Lingard et al. \(2020\)\]](#) were shown

to volunteers again in a repeat *validation subset* in order to create a second aggregate model used to test internal consistency. We combine the classifications of galaxies in this *validation subset* with the original classifications. Clustering of drawn spiral arms and cleaning of points was then performed as detailed in [[Lingard et al. (2020)]]. We remove any galaxies for which fewer than two spiral arms were identified, as these do not provide our model with any information about inter-arm scatter. This results in a hierarchical data structure of 91 galaxies, 211 spiral arms and 215,678 points.

Spiral arm points are deprojected to a face-on orientation using the disk inclination and position angle obtained through photometric model fitting performed in [[Lingard et al. (2020)]]. Arms are individually corrected to all have the same chirality (a pitch angle greater than or equal to zero) using the logarithmic spiral fit in [[Lingard et al. (2020)]].

### 2.3 Bayesian modelling of spiral arms in *Galaxy Builder*

We assume that a galaxy has a single value for pitch angle,  $\phi_{\text{gal}}$ , and that the pitch angles of spiral arms in this galaxy,  $\phi_{\text{arm}}$ , are constants (giving logarithmic spirals) drawn from a normal distribution centred on  $\phi_{\text{gal}}$ , with some spread  $\sigma_{\text{gal}}$  common to all galaxies. We truncate this normal distribution between the physical limits of  $0^\circ$  (a ring) and  $90^\circ$  (a “spoke”), giving

$$\phi_{\text{arm}} \sim \text{TruncatedNormal}(\phi_{\text{gal}}, \sigma_{\text{gal}}, \text{min} = 0, \text{max} = 90). \quad (3)$$

Furthermore, we assume that the observed points in a *Galaxy Builder* spiral arm, once deprojected, follow a logarithmic spiral with gaussian radial error  $\sigma_r$ ,

$$\widetilde{r_{\text{arm}}} = \exp\left(\overrightarrow{\theta_{\text{arm}}} \tan \phi_{\text{arm}} + c_{\text{arm}}\right). \quad (4)$$

Where  $\widetilde{r_{\text{arm}}}$  is the model’s predictions for the radii of the deprojected points in a *Galaxy Builder* arm ( $\overrightarrow{r_{\text{arm}}}$ ), and  $\overrightarrow{\theta_{\text{arm}}}$  is the polar angles of the points.

We choose hyperpriors over  $\phi_{\text{gal}}$ ,  $\sigma_{\text{gal}}$ ,  $c_{\text{arm}}$  and  $\sigma_r$  of

$$\phi_{\text{gal}} \sim \text{Uniform}(\text{min} = 0, \text{max} = 90), \quad (5)$$

$$\sigma_{\text{gal}} \sim \text{InverseGamma}(\alpha = 2, \beta = 20), \quad (6)$$

$$c_{\text{arm}} \sim \text{Cauchy}(\alpha = 0, \beta = 10), \quad (7)$$

$$\sigma_r \sim \text{InverseGamma}(\alpha = 2, \beta = 0.5). \quad (8)$$

The inverse gamma distribution is used to aid the convergence of the Hamiltonian Monte Carlo algorithm used (discussed later). The Cauchy distribution is equivalent to the Student’s t-distribution with one degree of freedom, and was chosen due to its fatter tails than the normal distribution. Our likelihood function for  $N$  arms, each of which with  $n_{\text{arm}}$  points is

$$\mathcal{L} = \prod_{\text{arm}=1}^N \left(2\pi\sigma_r^2\right)^{-n_{\text{arm}}/2} \exp\left(-\frac{\|\overrightarrow{r_{\text{arm}}} - \widetilde{r_{\text{arm}}}\|^2}{2\sigma_r^2}\right). \quad (9)$$

To perform inference, we make use of the No-U-Turn-Sampler (NUTS, Hoffman & Gelman 2011), implemented in PYMC3<sup>1</sup>, an open source probabilistic programming framework written in python (Salvatier et al. 2016). To aid the convergence of MC chains, we scale the radii of deprojected points to have unit variance.

## 3 RESULTS

### 3.1 Constraints on Galaxy Pitch angle

Our hierarchical model identifies the pitch angle of individual arms ( $\phi_{\text{arm}}$ ) with less than  $1.6^\circ$  of uncertainty for 95% of arms, assuming no error on disc inclination and position angle. The pitch angle of a galaxy as a whole ( $\phi_{\text{gal}}$ ), however, is not well constrained. This is primarily a result of only having pitch angles measurements for a small number of arms per galaxy, and reflects the difficulty in providing a single value for the pitch angle of a galaxy containing individual arms with very different pitch angles. For galaxies with two arms identified in *Galaxy Builder*, we have a mean uncertainty of ( $\sigma_{\phi_{\text{gal}}}$ ) of  $7.8^\circ$ , which decreases to  $6.7^\circ$  and  $5.8^\circ$  for galaxies with three and four arms respectively. This is consistent with the standard error on the mean for a galaxy with  $N$  arms,

$$\sigma_{\phi_{\text{gal}}} = \frac{\sigma_{\phi_{\text{arm}}}}{\sqrt{N}}, \quad (10)$$

where  $\sigma_{\phi_{\text{arm}}}$  is our measure of inter-arm variability of pitch angle and has a posterior distribution of  $11.0^\circ \pm 1.0^\circ$ . This variability is similar to the finding of Davis & Hayes (2014) and emphasises the need for fitting algorithms to not assume all arms have the same pitch angle.

### 3.2 Dependence of pitch angle on Galaxy Morphology

In order to test the possible progenitor distribution of our estimated arm pitch angles, we repeatedly perform an Anderson-Darling test (Stephens 1974) over each draw present in the MC trace, resulting in a distribution of Anderson-Darling statistics. We will refer to this test as the *marginalized Anderson-Darling test*. We also make use of the two-sample Anderson-Darling (Scholz & Stephens 1987) and Kolmogorov-Smirnov tests in a similar manner for comparison.

#### 3.2.1 Pitch angle vs. Bulge size

We define a bulge prominence from Galaxy Zoo 2 as Equation 3 in Masters et al. (2019):

$$B_{\text{avg}} = 0.2p_{\text{justnoticeable}} + 0.8p_{\text{obvious}} + 1.0p_{\text{dominant}}. \quad (11)$$

We see no correlation between galaxy pitch angle derived from the hierarchical model and  $B_{\text{avg}}$ . The Pearson correlation coefficient between the expectation value of galaxy

<sup>1</sup> <https://docs.pymc.io/>

pitch angle ( $E(\phi_{\text{gal}})$ ) and  $B_{\text{avg}}$  is -0.09. We see a slight correlation between  $E(\phi_{\text{gal}})$  and the fraction of volunteers who said a galaxy did not have a bulge (Pearson correlation coefficient of 0.19).

**[[Do we need to do an Anderson-Darling test here?]]**

We separate our sample into “weaker bulged galaxies” and “stronger bulged galaxies” using , in order to examine whether they could be drawn from significantly different distributions. A marginalized two-sample Anderson-Darling test does not find any evidence that the samples were drawn from different distributions; we do not reject the null hypothesis at the 1% level for any samples. The distribution of Anderson-Darling test statistics is shown in the upper panel of Figure 1.

### 3.2.2 Pitch angle vs. Bar Strength

We see no correlation between galaxy pitch angle derived from the *hierarchical normal model* and Galaxy Zoo 2’s debiased  $pbar$ , which is widely viewed as a good measure of bar strength, and therefore a measure of the torque applied on the disc gas.

Separating the sample based off of  $pbar > 0.5$ , and restricting to galaxies with more than 10 classifications for  $pbar$  (as performed by Masters et al. 2011 and Kruk et al. 2017) and performing a marginalized two-sample Anderson-Darling test does not find that the samples were drawn from different distributions (we reject the null hypothesis at the 1% level for only 1% of samples). The distribution of Anderson-Darling test statistics is shown in the lower panel of Figure 1.

We do not account for variation in bulge size in this work, however predictions from Manifold theory should not be affected as bulges do not provide a non-axisymmetric focusing.

## 3.3 Spiral Winding

For transient and recurrent spiral arms driven by self-gravity, Pringle & Dobbs (2019) suggest that spiral patterns form at some maximum pitch angle ( $\phi_{\text{max}}$ ), continually wind up over time and finally dissipate at some minimum pitch angle ( $\phi_{\text{min}}$ ). They propose that, under a set of very simple assumptions, the evolution of pitch angle would be governed by

$$\cot \phi = \left[ R \frac{d\Omega_p}{dR} \right] (t - t_0) + \cot \phi_{\text{max}}, \quad (12)$$

where  $\Omega_p$  is the radially dependant pattern speed of the spiral arm and  $t_0$  is the initial time at which it formed.

In QSDW theory, the pattern speed  $\Omega_p$  is a constant in  $R$ , as spiral arms obey rigid-body rotation. If  $\Omega_p$  instead varies with radius we would expect  $\cot \phi$  to be uniformly distributed between  $\cot \phi_{\text{max}}$  and  $\cot \phi_{\text{min}}$ .

In order to test this theory, Pringle & Dobbs (2019) used a Kolmogorov-Smirnov test to examine the consistency of a sample of observed galaxy pitch angles with one uniform in  $\cot$ . Pitch angles were measured using discrete fourier transformations in one- and two-dimensions, and as such do not account for inter-arm variations. They chose limits of

$\cot \phi \in [1.00, 4.75]$  (roughly  $11.9^\circ < \phi < 45.0^\circ$ ), motivated by examination of their data.

We aim to replicate their work here, using our sample and methods. We will make use of the marginalized tests described above, and examine winding on a per-arm basis, as well as a per-galaxy basis. Observation of the distribution of arm pitch angles in our sample suggests limits of  $15^\circ < \phi < 50.0^\circ$ .

### 3.3.1 Galaxy Pitch angle

Testing the uniformity in  $\cot$  of  $\phi_{\text{gal}}$ , between the limits specified above, using a marginalized Anderson-Darling test, results in rejecting the null hypothesis at the 1% level for 68% of samples. This suggests that a cot uniform model is not a good fit to galaxy pitch angle, but is not conclusive enough for us to unilaterally reject winding governed by Equation 12. The full distribution of Anderson-Darling statistics can be seen in the upper panel of Figure 2.

This inconclusive result is perhaps unsurprising; were we to assume that spiral arms are transient and recurrent instabilities, there is little reason for all of the arms to be at precisely the same evolutionary stage at the same time. This is supported by the large spread in inter-arm pitch angles.

### 3.3.2 Arm Pitch angle

If we assume that spirals form and wind independantly in a galaxy and that their evolution over time can be described by Equation 12, the distribution of pitch angles of individual arms should be uniform in  $\cot$  between our limits.

Using the marginalized Anderson-Darling test we cannot reject the null hypothesis at the 10% level for any of the possible realizations of arm pitch angle. The resulting distribution of Anderson-Darling statistics in the lower panel of Figure 2. This result is highly consistent with the model for spiral winding proposed by Pringle & Dobbs (2019), and can be seen as evidence that spirals are formed through local disc perturbations, and are primarily governed by local forces.

This result is highly sensitive to the lower limit of  $\phi_{\text{gal}}$  chosen; decreasing it to  $10^\circ$  results in us rejecting the cot-uniform progenitor at greater than the 0.1% level for every realization of the posterior. As we have no information available on the biases present in *Galaxy Builder* spiral arm classification, we should use the higher limits.

**[[We do not account for observation effects, instead assuming that galaxy builder spiral arms are equally likely to be identified and recovered at all pitch angles. We also assume that the galaxy builder is representative of the general spiral population, which is not necessarily the case]]**

## 4 DISCUSSION

This paper presents a new Bayesian approach to estimate galaxy pitch angle, making use of citizen science results to measure spiral arms through photometric modelling. We introduce an adaptation of the Anderson-Darling test to incorporate full Bayesian posterior probabilities and utilize this test to investigate theories governing spiral formation and evolution.

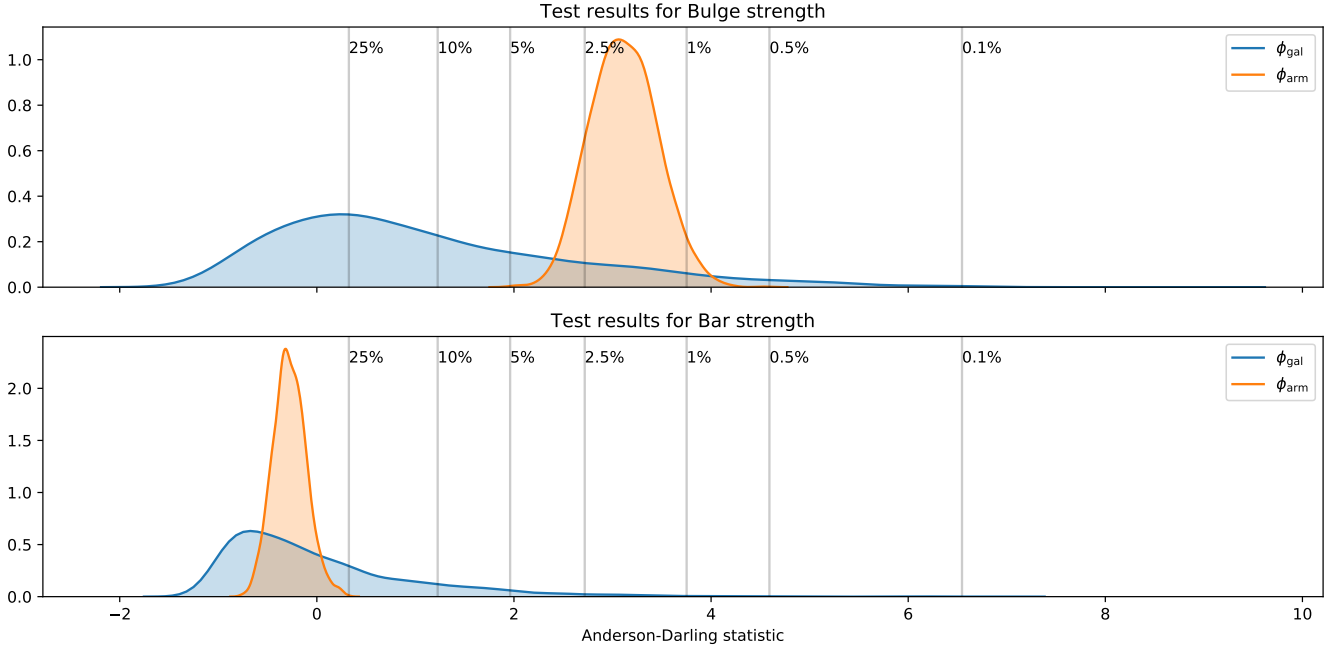


**Figure 1.** The results of marginalized two-sample Anderson-Darling tests examining whether pitch angles for Bulge-dominated and Disc-dominated galaxies are drawn from the same distribution (top panel), and the results of the same test for strongly-barred vs unbarred galaxies (bottom panel).

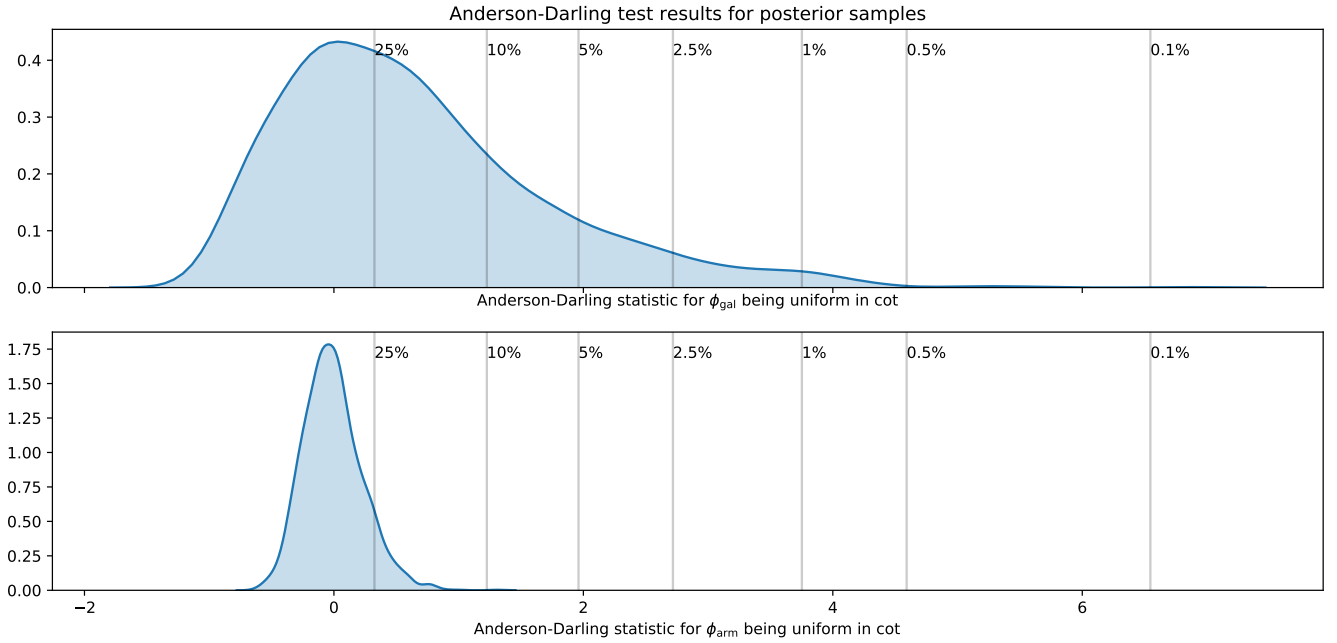


**Figure 2.** The results of a marginalized Anderson-Darling test for uniformity in cot for  $\phi_{\text{gal}}$  (top panel) and  $\phi_{\text{arm}}$  (bottom panel), with values corresponding to various confidence intervals shown. Moving rightwards on the x-axis implies greater confidence in rejecting the null hypothesis.

The statistical approach implemented in this paper allows a more thorough examination of pitch angle than simpler methods of logarithmic spiral fitting, and better accounts for inter-arm pitch angle variation than Fourier analysis, which assumes all arms in a given mode have the same pitch angle.

We do not find a relationship between bar strength and pitch angle, as would have been predicted by Manifold theory, and do not find evidence for the relationship between central mass concentration and pitch angle predicted by the Hubble sequence.

Our results are consistent with spiral winding of the form described by Pringle & Dobbs (2019); providing evidence for transient and recurrent spiral arms, the evolution of which is governed by self-gravity (such as through swing-amplification, Goldreich & Lynden-Bell 1965)) and which wind up over time. The assumptions of this model of spiral winding are also highly reductionist, and leaves many unanswered questions: what determines the limits on  $\phi$ ? Is the spiral arm equally apparent at all pitch angles, or is a selection effect present? This result is not evidence against QSDW, as it is possible that our distribution of pitch angles is dictated by other factors such as disk shear and central mass concentration.

As with most analyses, the most impactful improvement it would be possible to make here would be to increase the cleanliness and volume of data analysed; due to time constraints the *Galaxy Builder* galaxies used are not guaranteed to be representative. However, we believe that the methodology proposed here is a scalable, robust solution to the problems facing investigation of spiral morphology.

## 5 ACKNOWLEDGEMENTS

This publication made use of SDSS-I/II data. Funding for the SDSS and SDSS-II was provided by the Alfred P. Sloan Foundation, the Participating Institutions, the National Science Foundation, the U.S. Department of Energy, the National Aeronautics and Space Administration, the Japanese Monbukagakusho, the Max Planck Society, and the Higher Education Funding Council for England. The SDSS Web Site is <http://www.sdss.org/>.

This publication uses data generated via the Zooniverse.org platform, development of which is funded by generous support, including a Global Impact Award from Google, and by a grant from the Alfred P. Sloan Foundation. We would also like to thank the 2,340 volunteers who have submitted classifications to the *Galaxy Builder* project, especially user EliabethB, whose presence on the *Galaxy Builder* forum on top of a large number of galaxies modelled has been a huge help.

This project was partially funded by a Google Faculty Research Award to Karen Masters (<https://ai.google/research/outreach/faculty-research-awards/>), and Timothy Lingard acknowledges studentship funding from the Science and Technology Facilities Council (ST/N504245/1).

## References

- Athanassoula E., Romero-Gómez M., Masdemont J. J., 2009a, *MNRAS*, 394, 67
- Athanassoula E., Romero-Gómez M., Bosma A., Masdemont J. J., 2009b, *MNRAS*, 400, 1706
- Baba J., Saitoh T. R., Wada K., 2013, *ApJ*, 763, 46
- Binney J., Tremaine S., 1987, *Galactic dynamics*
- Blanton M. R., Kazin E., Muna D., Weaver B. A., Price-Whelan A., 2011, *AJ*, 142, 31
- Buta R., 1989, *Galaxy Morphology*. p. 151
- Buta R. J., et al., 2015, *VizieR Online Data Catalog*, p. J/ApJS/217/32
- Davis B., 2015, PhD thesis, University of Arkansas
- Davis D. R., Hayes W. B., 2014, *ApJ*, 790, 87
- Davis B. L., Berrier J. C., Shields D. W., Kennefick J., Kennefick D., Seigar M. S., Lacy C. H. S., Puerari I., 2012, *ApJS*, 199, 33
- Davis B. L., Graham A. W., Seigar M. S., 2017, *MNRAS*, 471, 2187
- Díaz-García S., Salo H., Knapen J. H., Herrera-Endoqui M., 2019, *arXiv e-prints*, p. arXiv:1908.04246
- Dobbs C., Baba J., 2014, *Publ. Astron. Soc. Australia*, 31, e035
- Elmegreen D. M., et al., 2011, *ApJ*, 737, 32
- Gao H., Ho L. C., 2017, *ApJ*, 845, 114
- Goldreich P., Lynden-Bell D., 1965, *MNRAS*, 130, 125
- Grand R. J. J., Kawata D., Cropper M., 2012, *MNRAS*, 426, 167
- Hart R. E., et al., 2017, *MNRAS*, 472, 2263
- Herrera-Endoqui M., Díaz-García S., Laurikainen E., Salo H., 2015, *A&A*, 582, A86
- Hewitt I. B., Treuthardt P., 2020, *MNRAS*, 493, 3854
- Hoffman M. D., Gelman A., 2011, *arXiv e-prints*, p. arXiv:1111.4246
- Hubble E. P., 1926, *ApJ*, 64, 321
- Julian W. H., Toomre A., 1966, *ApJ*, 146, 810
- Kormendy J., Kennicutt Robert C. J., 2004, *ARA&A*, 42, 603
- Kruk S. J., et al., 2017, *MNRAS*, 469, 3363
- Lin C. C., Shu F. H., 1964, *ApJ*, 140, 646
- Lintott C. J., et al., 2008, *MNRAS*, 389, 1179
- Mark J. W. K., 1976, *ApJ*, 205, 363
- Masters K. L., et al., 2011, *MNRAS*, 411, 2026
- Masters K. L., et al., 2019, *MNRAS*, 487, 1808
- Mutlu-Pakdil B., Seigar M. S., Hewitt I. B., Treuthardt P., Berrier J. C., Koval L. E., 2018, *MNRAS*, 474, 2594
- Peng C. Y., Ho L. C., Impey C. D., Rix H.-W., 2010, *AJ*, 139, 2097
- Pringle J. E., Dobbs C. L., 2019, *arXiv e-prints*, p. arXiv:1909.10291
- Rodriguez-Fernandez N. J., Combes F., 2008, *A&A*, 489, 115
- Romero-Gómez M., Masdemont J. J., Athanassoula E., García-Gómez C., 2006, *A&A*, 453, 39
- Salvatier J., Wiecki T. V., Fonnesbeck C., 2016, *PeerJ Computer Science*, 55
- Sandage A., 1961, *The Hubble Atlas of Galaxies*
- Sanders R. H., Huntley J. M., 1976, *ApJ*, 209, 53
- Savchenko S. S., Reshetnikov V. P., 2013, *MNRAS*, 436, 1074
- Scholz F. W., Stephens M. A., 1987, *Journal of the American Statistical Association*, 82, 918
- Seigar M. S., Block D. L., Puerari I., Chorney N. E., James P. A., 2005, *MNRAS*, 359, 1065
- Stephens M. A., 1974, *Journal of the American Statistical Association*, 69, 730
- Willett K. W., et al., 2013
- Yoshizawa M., Wakamatsu K., 1975, *A&A*, 44, 363
- Yu S.-Y., Ho L. C., 2019, *ApJ*, 871, 194
- de Vaucouleurs G., de Vaucouleurs A., Corwin Herold G. J., Buta R. J., Paturel G., Fouque P., 1991, *Third Reference Catalogue of Bright Galaxies*

Appendix

This paper has been typeset from a  $\text{\TeX}$ / $\text{\LaTeX}$  file prepared by the author.